Proceedings of the ASME 2013 Pressure Vessels & Piping Division Conference
PVP2013
July 14-18, 2013, Paris, France

PVP2013-97183

CONSTRUCTING A VALIDATED DEFORMATION MECHANISM MAP USING LOW TEMPERATURE CREEP STRAIN ACCOMMODATION PROCESSES FOR WASPALOY (A NICKEL-BASED SUPERALLOY)

Mahyar Asadi [*],
masadi@uottawa.ca
Dominic Guillot,
dguil071@uottawa.ca
Arnaud Weck
aweck@uottawa.ca

Mechanical Eng. Dept.
the University of Ottawa
Ottawa, ON, K1N 6N5
Canada

Ashok K. Koul
koula@lifepredictiontech.com

Life Prediction Technologies
1010 Polytek Street
Ottawa, ON, K1J 9J1
Canada

Ahmad Chamanfar,
achamanfar@gmail.com
Mohammad Jahazi
Mohammad.Jahazi@etsmtl.ca

Departement de Genie Mecanique
Ecole de Technologie Superieure
Montreal, QC, H3C 1K3
Canada

ABSTRACT

A creep Deformation Mechanism Map (DMM) of an engineering alloy can be an effective tool for developing physics based prognostics systems. Many classical diffusion based rate equations have been developed for time dependent plastic flow where dislocation glide, dislocation glide-plus-climb and vacancy diffusion driven grain boundary migration (diffusion creep) are rate controlling. Long term creep testing and analysis of complex engineering alloys has shown that power law breakdown phenomenon is related to the dominance of Grain Boundary Sliding (GBS) as opposed to diffusion creep. Rate equations are now available for GBS in complex alloys and, in this paper, a DMM is constructed for Waspaloy (a Nickel-Based Superalloy) and validated by comparison with a collection of experimental data obtained from the literature. The GBS accommodated by wedge type cracking is considered dominant at low homologous temperatures (0.3 to 0.5Tm - temperature in Kelvin) whereas GBS accommodated by power-law or cavitations creep dominates above 0.55Tm.

NOMENCLATURE

DMM: Deformation Mechanisms Map.
GBS: Grain Boundary Sliding.
PLC: Power Law Creep.
PLB: Power Law Breakdown.
IG: Intra-Granular.
W-Type: Wedge type cracking.
R-type: Cavitation type Cracking.
4D: 4 Dimensional.
T_m: Melting Temperature in Kelvin.
$\frac{T}{T_m}$: Homologous Temperature.
$\frac{\sigma}{\sigma_0}$: Normalized Stress.

INTRODUCTION

Complex engineering alloys that are used for high temperature applications such as Waspaloy, are typically precipitation-hardened and their grain boundaries are also strengthened using selective carbide precipitation mechanisms. Their grain sizes are also carefully controlled. The primary objective of using these

[*](Correspondence Author, cross-affiliation with Materials Eng. Dept. The University of British Columbia, Vancouver, B.C. V6T 1Z4, Canada)

microstructural design concepts is to optimize their high temperature yield strength as well as creep properties. Waspaloy is widely used in the industry for high temperature applications in aircraft as well as land-based gas turbine engines. Time and temperature dependence of creep strain accumulation and formation of a creep crack are the main design criteria used in practice for this class of materials.

Practical range of creep analysis requires the availability of creep data in the strain rate range of 10^{-8} to 10^{-10}/s and a temperature range of 0.3 to 0.7 Tm . Most academic creep studies on complex engineering alloys have focused on short term creep response because it is expedient to generate the creep data and extrapolation techniques in combination with theoretical treatments developed for simple metals and alloys have been employed to predict the long term creep response of these alloys. In contrast, long term creep studies carried out by the industry have limited their analysis using empirical modeling techniques. This divide between the academia and the industry led studies has created a lot of confusion in understanding the creep deformation phenomenon of complex engineering alloys.

EVOLUTION OF COMPLEX ALLOY DMM

The creep deformation is essentially a time dependent and thermally activated plastic strain accumulation processes that are controlled by the competition between the activation energies associated with different mechanisms such as dislocation glide and climb within the grain interiors (Power-Law Creep - PLC) or at the grain boundaries (GBS) or stress assisted vacancy migration leading to grain boundary migration (diffusion creep). All of these processes occur at the atomic scale over time and often lead to time dependent plastic strain accumulation at stresses that are well below the temperature dependent yield strength of the material.

The constitutive equations for creep define the creep strain-rate as a function of applied stress, temperature and material microstructure (σ_t , T_t and S_t in Eq. 1 where t is the discretized time). It is now well recognized that the micrsotructure of the material itself evolves as creep strain continues to accumulate (Eq. 2) although most workers who have developed mathematical formulations for different creep deformation mechanisms tend to ignore this effect.

$$\frac{d\varepsilon}{dt} = f(\sigma_t, T_t, S_t) \tag{1}$$

$$\frac{dS}{dt} = f(\sigma, T, S) \tag{2}$$

Typical constitutive equations that have been developed for different creep deformation mechanisms for simple metals and alloys including some complex alloys are summarized in table 1. Frost and Ashby [1] developed a superposition method for combining different rate equations where one mechanism contributes dominantly to the total creep rate at a given stress and temperature while other mechanisms play a less significant role. This led to the development of a DMM which is a diagram that plots normalized stress and temperature and divided the two dimensional stress and temperature space into different regions in which a specific deformation mechanism remains dominant. Different creep strain rate contours are further superimposed on this space to provide a sense of strain rates over which a specific mechanism may dominate during the deformation process.

Mohammad and Langdon [2] created their own version of a DMM arguing that GBS, as opposed to Coble type diffusion creep, is likely to dominate at lower stresses because the overall energy barrier required for substantial grain boundary migration is quite large.

Koul and Castillo [3] conducted extensive creep testing on IN738LC turbine blade material with a grain size of 1.5 mm and microstructural studies on crept specimens and modified the DMM for a Ni-base superalloy by incorporating a GBS regime in a typical Ashby type DMM [4], [3], [5]. The transition between the PLC and GBS is obtained using experimental Power-Law Breakdown (PLB). They show that the GBS is the dominant mechanism within the practical range of land based and aircraft turbine operation. They further included an interface reaction controlled diffusion creep regime into the map assuming that, if diffusion creep is operative at very low stresses, the grain boundaries cannot act as perfect sources or sinks for vacancies in complex engineering alloys.

Wardsworth et. al. [6] have analyzed a vast amount of creep data that was available on different engineering alloys and concluded that GBS, as opposed to diffusion creep, was the dominant deformation mechanism in complex engineering alloys at lower stresses [7].

Recently, Banerjee et. al. [8] attempted to further subdivide the GBS dominant regime in a Ashby type DMM for a Pb-Sn eutectic solder alloy where the GBS region is further divided into two regions based on the dominance of different GBS accommodation processes. It is suggested that GBS is accommodated by w-type cracking below 0.5Tm whereas creep cavitation accommodation process is dominant above this temperature and this modification of the DMM is presented in Fig. 1 and served as template in this paper for developing DMM of Waspaloy.

Mechanisms	Rate Equation $[s^{-1}]$	Remarks
Dislocation Climb		
	$\dot{\varepsilon} = AD\frac{Gb}{kT}\left(\frac{\sigma}{G}\right)^{4.5}$	$A \simeq 10^6$
		G = shear Modulus
Diffusional Creep		
Nabarro-Herring (Bulk)	$\dot{\varepsilon} = BD\frac{Gb}{kT}\left(\frac{b}{d}\right)^2\left(\frac{\sigma}{G}\right)$	$B \simeq 30$
		$Threshhold\ Stress \simeq 10^{-7}G$
		$C \simeq 30$
Coble (Grain Boundary)	$\dot{\varepsilon} = CD\left(\frac{D_{GB}Gb}{kT}\right)\left(\frac{b}{d}\right)^2\left(\frac{\sigma}{G}\right)$	$B \simeq 30$
		$Threshhold\ Stress \simeq G\frac{b}{d}$
Ashby-Verrall	$\dot{\varepsilon} = FD\frac{b}{kT}\left(\frac{b}{d}\right)^2(\sigma-\sigma_1)\left[1+\frac{\delta}{d}\left(\frac{D_{GB}}{D}\right)\right]$	$F \simeq 100$
(Diffusional Accommodated Flow)		$Threshhold\ Stress \simeq G\frac{b}{d}$
		$\delta = GB\,thickness$
		$Threshhold\ Stress = \sigma_1 = \frac{0.7\Gamma}{d}$
		$\Gamma = GB\,free energy$
Grain Boundary Sliding		
Controlled by GB Diffusion	$\dot{\varepsilon} = HD_{gbs}\frac{Gb}{kT}\left(\frac{b}{d}\right)^2\left(\frac{\sigma}{G}\right)^2$	$H \simeq 8\times10^5$
Controlled by Lattice Diffusion	$\dot{\varepsilon} = LD\frac{Gb}{kT}\left(\frac{b}{d}\right)^2\left(\frac{\sigma}{G}\right)^2$	$L \simeq 10^7$
Haper-Dorn	$\dot{\varepsilon} = MD\frac{Gb}{kT}\frac{\sigma}{G}$	$M \simeq 10^{-11}$
Complex Engineering Alloy	$\dot{\varepsilon} = AD\frac{Gb}{kT}\left(\frac{b}{d}\right)^q\left(\frac{\lambda+r}{b}\right)^{q-1}\left(\frac{(\sigma-\sigma_{0glide})(\sigma-\sigma_{0climb})}{G^2}\right)$	$A \simeq 10^6$
(GBS in Presence of Precipitates)		$q = 1\,(without\ particles)$
		$q = 2\,(discrete\ particles)$
		$q = 3\,(continuous\ network\ of\ particles)$
		λ : $interledge\ spacing$
		r : $average\ grain\ boundary\ ledge\ height$

TABLE 1: VARIETY OF CREEP MECHANISMS AND FORMULA [9], Complex Eng. Alloy [10].

CONSTRUCTING A MODIFIED DEFORMATION MECHANISM MAP (DMM)

The construction of a practical DMM using numerical techniques requires the availability of long as well as short term creep test data in order to obtain the correct numerical output with respect to the experimental data over a wide range of temperatures and stress conditions. As pointed out earlier, it is not sufficient to perform creep tests at higher temperatures alone where creep rates are relatively higher and use some theoretical assumptions to construct the map. As a minimum, some test data should be available in the PLC and PLB regimes to capture the transition between the PLC and the GBS. The practical range of temperatures and stresses in the case of cast turbine blades is limited to a small region in the PLB regime.

As pointed out by Wardsworth et. al. [6], in complex engineering alloys, intense defect activity in the grain boundary plane and the adjacent regions during GBS takes place and strain accommodation processes in the form of precipitate denudation zones, minor migration and grain boundary cracking also remain active.

In the case of wrought alloys such as Waspaloy, it has been suggested that w-type cracking at the grain boundaries and grain boundary cavitation (r-type) are the main GBS strain accommodation processes [8], [11]. However, the possibility of a transition between the w-type and r-type strain accommodation processes as a function of stress and temperature has not been explored. There are currently only few (in some case none) experimental data bases available in the literature on creep tests at the relatively

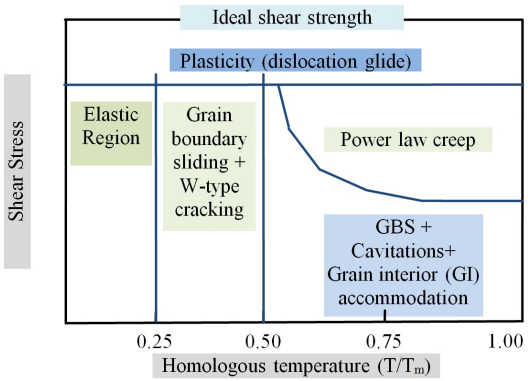

FIGURE 1: A MODIFIED DMM WITH GBS USED AS THE TEMPLATE FOR DEVELOPING WASPALOY'S DMM IN THIS PAPER [8].

lower temperatures ($0.5T_m$ or below) to observe the transition between the GBS accommodated by w-type and r-type cracking.

DATA COLLECTION

A fair amount of creep information is available in the literature for Waspaloy. An extensive literature survey was conducted to collect as much creep data as possible. The data collection exercise focused on the minimum creep rate which is the most critical design parameter that can be extracted from a constant load creep test from a life prediction perspective [12]. Values for creep strain rates were plotted for tests performed on samples with a grain size of approximately 40 μm as revealed in Fig. 2 [13]. In cases where grain size information was not available, it was assumed that the samples had received the conventional heat-treatment and the grain size lay in the range of 30 μm to 50 μm [14]. Eq. 3 was used to normalize the effect of grain size on the creep strain rate. In this equation, d_1 and d_2 denote grain sizes for two different creep rates. Since this equation lies in the GBS regime, the creep rates cannot be adjusted for creep experimental points in the dislocation glide regime.

Generally, each deformation mechanism leads to a different value of the stress exponent (n) in the Arrhenius-type creep equation [12]. Thus, this value can be used to identify the stress range in which a certain mechanism is dominant.

$$\dot{\varepsilon}_2 = \dot{\varepsilon}_1 \left(\frac{d_1}{d_2}\right)^2 \tag{3}$$

Fig. 3 shows a collection of experimentally measured minimum creep rates from different reliable sources including National Research Council of Canada (NRC) [15], Oak Ridge National Laboratory (ORNL) for Lockheed Martin [16], University of Nottingham [17], Denmark Riso National Laboratory and Germany Metallgesellschafi A G, Metall-Laboratorium [18]. These data are tested on fine granular Waspaloy and table 2 provides the values. The minimum creep rate values are converted to $[hr^{-1}]$ to conform with the computational results calculated in this paper.

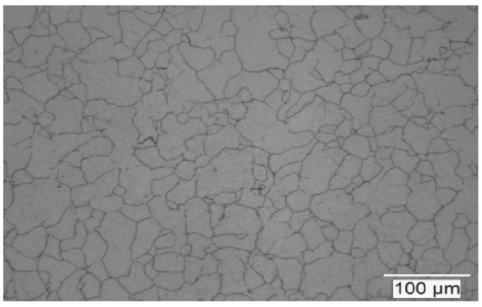

FIGURE 2: AVERAGE GRAIN SIZE OF 42 MICRON MEASURED FROM THE MICRO-STRUCTURE OF A WASPALOY SAMPLE THAT HAD RECEIVED THE CONVENTIONAL HEAT-TREATMENT [13].

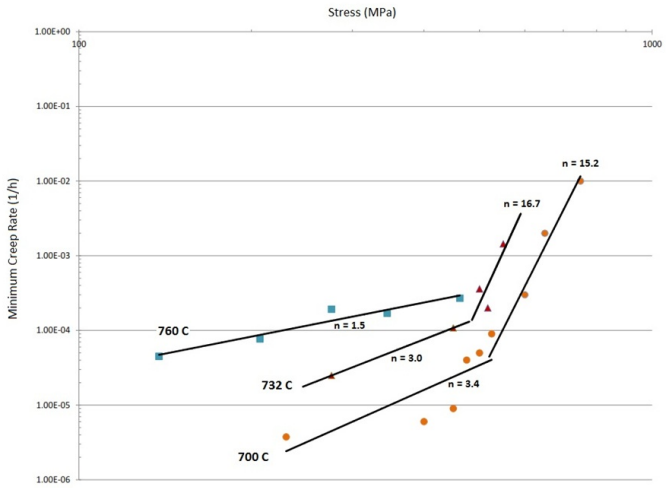

FIGURE 3: WASPALOY, PLOT OF MINIMUM CREEP RATE VS. STRESS SHOWING THE POWER-LAW BREAK-DOWN AT VARIOUS TEMPERATURES.

COMPUTATIONAL MODEL FOR DMM

A frequently-used model for creep strain rate around the PLB is the superposition of two strains that are grain boundary sliding and intragranular (IG) deformation (or dislocation glide-

Homologous Temperature	Normalized Shear Stress	Minimum Creep Rate	Reference
$T/T_m, T_m = 1600\ [^\circ K]$	$Log_{10}(\sigma/G_0), G_0 = 8.18\times10^5$ [MPa]	$[hr^{-1}]$	
0.61	-3.60	3.75×10^{-6}	[18]
0.61	-3.53	6.00×10^{-6}	[17]
0.61	-3.48	9.00×10^{-6}	[17]
0.61	-3.38	4.00×10^{-5}	[17]
0.61	-3.34	5.00×10^{-5}	[17]
0.61	-3.31	9.00×10^{-5}	[17]
0.61	-3.24	3.00×10^{-4}	[17]
0.61	-3.18	2.00×10^{-3}	[17]
0.61	-3.15	1.00×10^{-2}	[17]
0.63	-3.24	2.49×10^{-5}	[16]
0.63	-3.21	1.08×10^{-4}	[15]
0.63	-3.18	3.60×10^{-4}	[15]
0.63	-3.17	2.00×10^{-4}	[16]
0.63	-3.12	1.44×10^{-3}	[15]
0.65	-3.24	4.49×10^{-5}	[16]
0.65	-3.18	7.72×10^{-5}	[16]
0.65	-3.13	1.92×10^{-4}	[16]
0.65	-3.08	1.70×10^{-4}	[16]
0.65	-3.04	2.70×10^{-4}	[16]

TABLE 2: MINIMUM CREEP RATE EXPERIMENTALLY MEASURED AND REPORTED FOR WASPALOY.

plus-climb) as shown in Fig. 4. There is a variety of rate equations for grain boundary sliding and intragranular strain rates and, in this paper, the rate Eqs. 5 and 6 were initially used for GBS and IG (from table1). The constant coefficient and power values have then been modified to obtain a better agreement with the experimental data. The term σ in intragranular rate equation is the effective stress experienced by the dislocations and this is altered in [9] to $\sigma - \sigma_0$ where σ_0 is the friction stress or the internal stress inside the material, that is, the minimum stress required for dislocations motion process in a precipitation hardened alloy. The term σ_0 is associated with precipitation hardening [9] and set constant here because the precipitation's size and distribution are assumed unchanged during the creep process. The computational algorithm has been developed using the Open-source R-Project with standard package for computation, Lattice package, and 4D Contourplot for visualization.

$$\dot{\varepsilon} = \dot{\varepsilon}_{gbs} + \dot{\varepsilon}_{ig} \tag{4}$$

$$\dot{\varepsilon}_{gbs} = HD_{gbs}\frac{Gb}{kT}\left(\frac{b}{d}\right)^2\left(\frac{\sigma}{G}\right)^2 \tag{5}$$

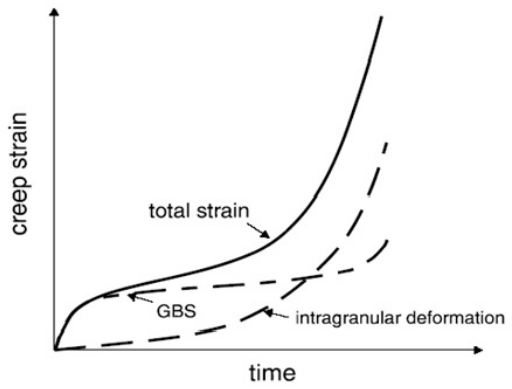

FIGURE 4: SUPERPOSITION CREEP MODEL AROUND THE POWER-LAW BREAK-DOWN REGION [19].

$$\dot{\varepsilon}_{ig} = AD_{ig}\frac{Gb}{kT}\left(\frac{\sigma - \sigma_0}{G}\right)^{4.5} \tag{6}$$

Table 3 shows the values employed for computationally developing the DMM including the references used in each case. Temperature-dependent diffusion coefficients (for both GBS and IG deformation) and shear modulus are used and updated in the rate equations for given temperatures. The relationships are given in Eqs. 7 [1], 8 [1], and 9 [20]. The temperature-dependent shear modulus equation is based on experimental measurements conducted by Farraro [20] for Young's modulus and converted to shear modulus using $\mu = E/2(1+\nu)$ where μ, E, and ν are shear modulus, Young's modulus, and Poisson ratio equal to 1/3 respectively.

Parameter	Notation	Value	Unit	Reference
Melting Temperature	T_m	1600	$^\circ K$	[19]
Burger Vector	b	2.5×10^{-4}	μm	[1]
Boltzman Constant	k	1.38×10^{-23}	$J/^\circ K$	[1]
Pre-exponent, Intragranular	D_{0v}	2×10^{-6}	m^2/s	[16]
Activation Energy, Intragranular	Q_v	545000	J/mol	[16]
Gas Constant	R	8.3144	$J/mol^\circ K$	[1]
Grain Size	d	40	μm	[13]
Friction Stress	σ_0	22×10^6	Pa	[9]
Pre-exponent, gbs	D_{0c}	$4b^2D_{0v}$	m^2/s	[1]
Activation Energy, gbs	Q_c	$0.6Q_v$	J/mol	[1]

TABLE 3: VALUES EMPLOYED IN COMPUTATION ALGORITHM [9].

$$D_{ig} = D_{0v} exp\left(\frac{-Q_v}{RT}\right) \tag{7}$$

$$D_{gbs} = D_{0c} exp\left(\frac{-Q_c}{RT}\right) \tag{8}$$

$$G = (88.75 - 0.0256T) \times 10^9 \ \ [Pa] \tag{9}$$

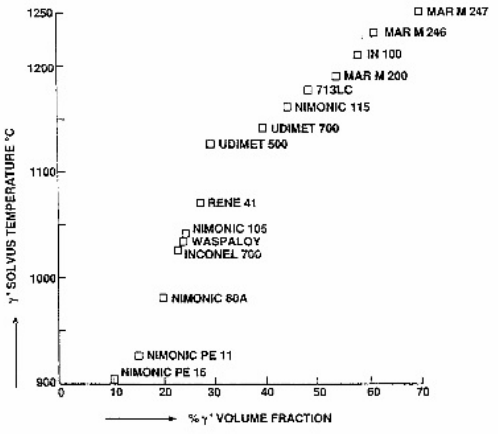

FIGURE 5: RELATION BETWEEN γ' volume fraction and $\gamma' - solvus$ TEMPERATURE FOR NI-BASE SUPERALLOY [5].

COMPUTATIONAL RESULTS AND EXPERIMENTAL DATA

The results of the predicted DMM are shown in Fig. 6 and the experimental data from table 2 are added to the plot as triangle symbol for comparison. The Y-axis is log-plot and the values are $Log(_{10}\frac{\sigma}{G_0})$. For example, the value -3.1 corresponds to 650 [MPa] calculated by $normalized\,shear\,stress = 10^{-3.1} = 0.000795$ then $\sigma = 0.000795 \times 818000[MPa] = 650[MPa]$ (G_0 is the shear modulus at 273 $^\circ K$ which is about 818,000 $[MPa]$). The points on the map are the rates given in table 2. Adding the experimental rate values beside the triangles on this plot makes it inconvenient to read. Readers may use table 2 for the experimental values. The error in experimental measurement that can be assessed by repeating the tests requires for a valid comparison. Although a typical creep test includes some experimental uncertainties, repeating the creep test is not common because the test takes too long. It should be mentioned that the computational results is deterministic and is comparable to the trend lines in Fig. 3 rather than the data points.

The slope of the trend lines added to the experimental data (log-plot in Fig. 3) suggests a modification to the n-power values in rate equations such that the power changes from 4.5 to 16 for the intragranular rate equation (dislocation climb), as well, from 2 to 3 for the grain boundary sliding rate equation. The constant coefficient has also changed for these equations from 10^6 to 5×10^{55} for the intragranular rate equation and from 8×10^5 to 8×10^{16} for the grain boundary sliding rate equation in order to develop a better prediction compared to the experimental data. The boundary between two regions; GBS and PLC is plotted presenting the transition from one mechanism to the other one. Further in this paper, the method to define this boundary has been explained in details. The Waspaloy is usually strengthened by the secondary phase precipitates. Fig. 5 presents $\gamma' - solvus$ temperature for different superalloys and this is abour 1030 $^\circ C$ for Waspaloy. Above the $\gamma' - solvus$ temperature, the basic nature of material completely changes due to dissolution of the major strengthening phase and therefore the rate equations can not be used. The vertical line at 0.82 homologous temperature on presented DMM shows the $\gamma' - solvus$ temperature.

Fig. 7 presents a 4D contour plot that visualizes two rate contours together. This helps understand the contribution from each mechanism to the total strain rate shown in Fig. 6 as well shows the transition boundary between the two mechanisms. The intersections between the black contours (GBS rate) and color contours (interagranular/climb) demonstrate the transition boundary between the two mechanisms where the dominant mechanism is switched from one to another. For example, if one follows the strain rate contour 10^{-5} on both GBS and IG contours, the intersection defines the transition boundary on which the GBS and PLC mechanisms are switched. This is based on the physical fact that the strain rates become equal on the transition boundary. A solid blue line that connects three circular points is added to this plot and shows the experimentally defined boundary from Fig 3.

CONCLUSION

A rationale and a methodology for developing practical Ashby type DMM has been created and summarized in this paper. Unlike in traditional Ashby type DMM, where diffusion creep is considered dominant at lower stresses and temperatures, GBS is considered to be the dominant deformation mechanisms below the PLB point as a function of stress and temperature. The GBS regime is further subdivided into w-type and r-type cracking accommodation processes for wrought alloys.

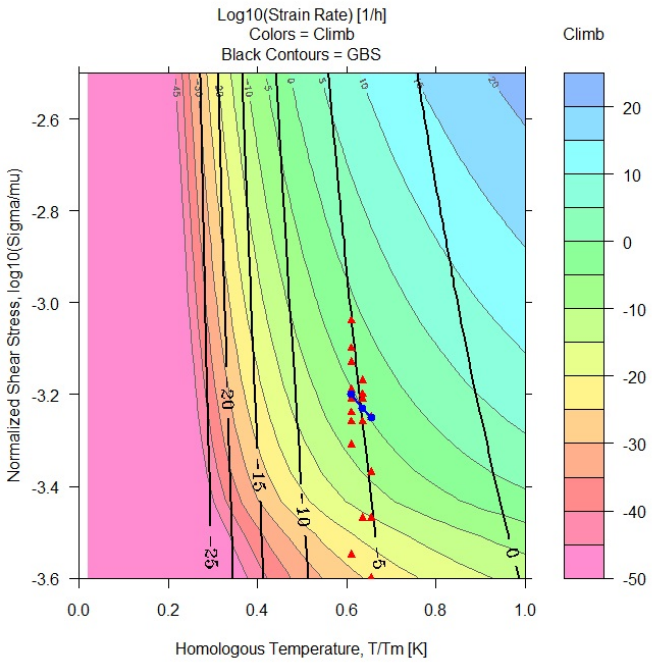

FIGURE 6: COMPUTATIONAL DMM DEVELOPED AND COMPARED TO THE EXPERIMENTAL DATA.

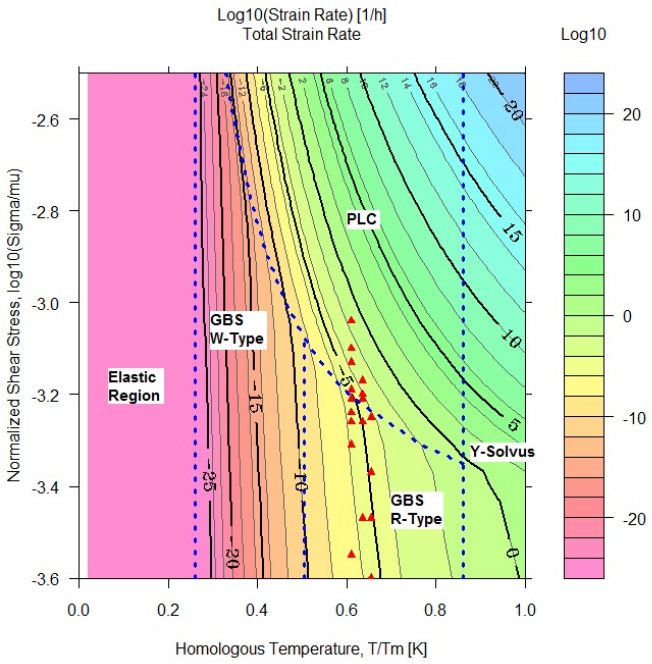

FIGURE 7: 4D CONTOUR PLOT THAT VISUALIZES TWO RATE CONTOURS AT THE SAME TIME FOR COMPARISON BETWEEN THE CONTRIBUTIONS FROM EACH MECHANISM.

A comparison between the modified Ashby type DMM and experimental data obtained from the literature indicates that Eq. 10 along with Eq. 7, 8, and 9 can accurately predict the creep rates for Alloy718.

$$\begin{aligned} \dot{\varepsilon} &= \dot{\varepsilon}_{gbs} + \dot{\varepsilon}_{ig} \\ \dot{\varepsilon}_{gbs} &= 8 \times 10^{16} D_{gbs} \frac{Gb}{kT} \left(\frac{b}{d}\right)^2 \left(\frac{\sigma}{G}\right)^3 \\ \dot{\varepsilon}_{ig} &= 5 \times 10^{55} D_{ig} \frac{Gb}{kT} \left(\frac{\sigma - \sigma_0}{G}\right)^{16} \end{aligned} \tag{10}$$

Although a grain size term appears in this relationship, the effect of grain size was not compared to the experimental data and this relationship is valid for grain sizes ranging between 30 to 50 μm. Further work will be required to study the effect of grain size.

The power value i.e. slope in log-log plot approximates constant for each rate equation, The experimental data shows that the power values tends to vary, for example from 1.5 to 3.4, in the grain boundary sliding rate equation. One may modify the equation for better prediction using variable power value.

This DMM can be used for creep life predictions of Waspaloy in ranges of temperatures and stresses used in practical applications, as well as to design experimental creep test matrices for wider ranges of stresses and temperatures.

ACKNOWLEDGMENT

The authors would like to thank Carpenter Technology Corporation for generously providing the University of Ottawa with Superalloy disk samples, as well as the financial support under the FedDev grant by the Canadian Federal Economic Development Agency for Southern Ontario.

REFERENCES

[1] H. J. Frost, M. F. Ashby, "*Deformation- Mechanism Maps; the Plasticity and Creep of Metals and Ceramics*", Book, Pergamon Press, ISBN 0-08-029338-7, 1982.

[2] F. A. Mohamed and T. G. Landgon, "*Deformation-Mechanism Maps; the Plasticity and Creep of Metals and Ceramics*", Book, Pergamon Press, ISBN 0-08-029338-7, 1982.

[3] A. K. Koul, R. Castillo, "*Creep Behavior of Industrial Turbine Blade Materials*", Proceeding of ASM Materials Congress Materials Week 93, Pittsburgh, Pennsylvania, 1993.

[4] A. K. Koul, Castillo and J. P. Immarigeon an, "*Superalloys Book*", TMS-AIME, 1988.

[5] A. K. Koul, J. P. Immarigeon, W. Wallace, "*Microstructural Control in Ni-Base Superalloys,In Advances in High Temperature Structural Materials and Protective Coatings*", National Research Council of Canada, 95-125, 1994.

[6] J. Wardsworth, O. Ruano, O. Sherby, "*Denuded Zones, Diffusional Creep, and Grain Boundary Sliding*", Metallurgical and Materials Transactions A, Chemistry and Materials Science, 33(2), 219-229, 2002.

[7] X. Wu, "*Life Prediction of Gas Turbine Materials*", Institute for Aerospace Research, National Research Council Canada, 2005.

[8] A. Banerjee, A. Koul, A. Kumar, N. Goel, "*Physics Based Prognostics of Solder Joints in Avionics*", Annual Conference of the Prognostics and Health Management Society, 2011.

[9] A. Lasalmonie, J. L. Strudel, "*Influence of Grain Size on the Mechanical Behaviour of Some High Strength Materials*", Journal of Materials Science 21, 1837-1852, 1986.

[10] X. J. Wu, A. K. Koul, "*Grain Boundary Sliding in the Presence of Grain Boundary Precipitates during Transient Creep*", Metallurgical and Material Transaction A, Volume 26A 905, 1995.

[11] A. Koul, "*Collaboration Report on Inconel 718 Project Status*", Internal Document, Life Prediction Technologies Inc., Ottawa, 2011.

[12] William, D. Callister, "*Materials Science and Engineering; An Introduction*", Book, 7th edition, Willey, 2007.

[13] A. Chamanfar, M. Jahazi, J. Gholipour, P. Wanjara, S. Yue, "*Suppressed Liquidation and Microcracking in Linear Friction Welded WASPALOY*",Materials and Design, 36, 113-122, 2012.

[14] R. Thamburaj, A. K. Koul, W. Wallace and M. C. De Malherbe, "*Effect of Microstructure and Environment on the Elevated Temperature Creep and Low Cycle Fatigue Crack Growth Rates in Inconel 718*", Laboratory Technical Report, National Research Council of Canada, 1986.

[15] N. K. Sinha, "*Stress Exponent and Primary Creep Parameters Using Single Specimen and Strain Relaxation and Recovery Test*", Materials Science and Engineering A 510-511, 450-456, 2009.

[16] C. G. McKamey, E. P. George, C. T. Liu, J. A. Horton, C. A. Carmichael, R. L. Kennedy, W. D. Cao, "*Manufacturing on Nickel-Base Superalloys with Improved High Temperature Performance*", Oak Ridge National Laboratory, Lockheed Martin, 2000.

[17] T. H. Hyde, L. Xia, A. A. Becker, W. Sun, "*Fatigue, Creep and Creep/Fatigue Behaviour of a Nickel Base Superalloy at 700 °C*", Fatigue Fract. Engng Mater. Struct. Vol. 20, No. 9, pp. 1295-1303, 1997.

[18] G. I. Rosen, S. F. Dirnfeld, M. Bamberger, A. Rosen, B. Prinz, "*Creep Investigation of Commercial and Improved Nickel-Based Wrought Superalloys*", Materials Science and Engineering, A 172, 15- 21, 1993.

[19] R. W. Evans, B. Wilshire, "*Creep of Metals and Alloys*", The Institute of Metals, London, pp. 314, 1985.

[20] R. Farraro, R. B. McLellan, "*Temperature Dependence of the Young's Modulus and Shear Modulus of Pure Nickel, Platinum, and Molybdenum*", Metallurgical Transactions A, Volume 8A, p 1565, 1977.